Engineered Science
DOI: https://dx.doi.org/10.30919/es1270

Optimizing Aggregate Selection and Mineral Additive to Enhance the Elasto-Mechanical Aspects of High-Performance Concrete

Shaik Numan Mahdi,[1] Kiran Kolambekodi,[2,*] Ragupathy Arul,[2] Aniket Vasantrao Kataware,[3] Nithiwach Nawaukkaratharnant,[1, 4,*] and Brabha Nagaratnam[5]

Abstract

This study focuses on deciphering the key factors influencing the production of high-performance concrete, with an emphasis on achieving elevated the mechanical properties of normal concrete (NC) and mineral admixture concrete (MAC). Through an extensive series of experiments, the investigation seeks to unravel the nuanced interplay of aggregate size, aggregate volume, and paste content in the quest for optimizing Young's modulus. The study utilized charnockite and hematite aggregate with varying maximum sizes, by incorporating fly ash (FA) and silica fume (SF) as mineral additives. The results revealed that the NC exhibits an increase in strength with the higher grade of M50 grade containing 20 mm aggregates (M 50/20). The MAC showed enhancements due to the use of mineral additives in heavy density concrete of 30 grade containing 20 mm aggregate (H 30/20). MAC H 30/20 showed significant strength improvements, with increases of 15.74% in split tensile strength, 26.05% in flexural strength, and 16.48% in compressive strength compared to NC M 50/20. Similarly, the Young's modulus was 40.16 GPa for the NC M 50/20 and 42.42 GPa for the MAC N 60/20. In summary, the study highlights the positive effects of hematite aggregates on concrete stiffness and the synergistic contributions of mineral additives.

Keywords: High-performance concrete; Stiffness; Young's modulus; Split tensile strength.
Received: 14 May 2024; Revised: 13 August 2024; Accepted: 08 October 2024.
Article type: Research article.

1. Introduction

In the field of structural engineering, Young's modulus or modulus of elasticity plays a pivotal role in ensuring the structural integrity and serviceability of concrete structures.[1] This fundamental property is extensively used for linear analysis, serving as a critical parameter in meeting both the ultimate and serviceability limit states of reinforced and prestressed concrete structures.[2,3] The significance of Young's modulus lies in its ability to calculate deflection and predict excessive deformation, thereby establishing a known threshold for the serviceability of concrete elements and facilitating the creation of economically optimized designs, especially in the field of high-strength concrete.[4] This study delves into the profound importance of Young's modulus in the construction industry, particularly emphasizing its role in defining high-performance concrete. In an era marked by the construction of unique and landmark buildings, the demand for high-performing concrete with elevated Young's modulus is burgeoning.[5,6] An integral aspect of our investigation involves meticulous consideration of locally available aggregates, balancing the need for economic viability with the pursuit of optimal concrete performance.[7-11] Recent research has shed light on the profound influence of aggregates on concrete, impacting stiffness,[12-15] mechanical properties, and dimensional stability. This becomes particularly crucial when striving for high elastic moduli, where aggregate volume, grain size, porosity, shape, surface texture, grading,

[1] *Metallurgy and Materials Science Research Institute, Chulalongkorn University, Bangkok 10330, Thailand.*
[2] *Department of Quality Assurance and Control, Larsen & Toubro Construction, Chennai 600001, India.*
[3] *Civil & Infrastructure Engineering, Indian Institute of Technology Dharwad, Karnataka 400076, India.*
[4] *Upcycled Materials from Industrial and Agricultural Wastes Research Unit, Department of Materials Science, Faculty of Science, Chulalongkorn University, Bangkok, 10330, Thailand.*
[5] *Department of Mechanical and Construction Engineering, University of Northumbria, Newcastle upon Tyne NE1 8ST, United Kingdom.*
**Email:* nithiwach.n@chula.ac.th (N. Nawaukkaratharnant), kirank@lntecc.com (K. Kolambekodi)

mineralogical composition, and rock crushing test results collectively shape the matrix and, consequently, the Young's modulus.[16-18]

Using volcanic tuffs of scoria as lightweight aggregates and replacing cement with 5 to 15% silica fume (SF) led to an increase of up to 14% in the Young's modulus compared to mixes without SF. In contrast, incorporating up to 10% fly ash (FA) as a partial cement replacement did not change the Young's modulus for these mixes. Additionally, the combination of 10% SF and 5% FA resulted in a notable increase in the Young's modulus compared to individual mixes containing the same proportions of either SF or FA.[19] The reduction in elastic modulus tends to decrease as the content of FA increases. Specifically, concrete containing 35% FA exhibited a reduction of up to 24% in elastic modulus when using 100% recycled aggregate.[20] The effective elastic modulus of concrete with recycled aggregates is lowered when recycled coarse aggregate (RCA) is included in the mixture. The degree of this reduction depends on the mechanical properties of the RCA, the amount used, and the design parameters of the concrete mix.[21] This reduction is primarily attributed to the presence of adhered old mortar in the RCA, which is softer than the aggregate itself, as well as potential mechanical damage sustained during the recycling process.[22,23]

Giaccio *et al*.[24] conducted the process by which coarse aggregate particles impede the growth of failure cracks, resulting in the formation of meandering and branching cracks, is elucidated. The impact of coarse aggregate on crack propagation is contingent upon specific aggregate characteristics, including surface texture, shape, and stiffness. It has been emphasized previously that the dissimilarity in elastic properties between the matrix and the aggregate plays a crucial role in influencing concrete failure. According to Giaccio *et al*.[25] the surface texture of the aggregate stands out as a key factor affecting matrix–aggregate bond strength, with rougher aggregates demonstrating superior bonding capabilities. Uysal *et al*.[26] delved into the impact of coarse aggregate types on the mechanical properties of self-compacting concrete (SCC). The study concluded that utilizing higher strength aggregates led to enhanced concrete strength. Additionally, Kilic *et al*.[27] highlighted a significant observation that concretes incorporating high compressive strength aggregates, such as gabbro and quartzite, exhibited lower compressive strength compared to the inherent strength of the aggregates. Conversely, concrete with lower strength aggregates like basalt, limestone, and sandstone results the compressive strength similar to the respective aggregates. The elastic modulus of concrete is directly correlated with the stiffness of its constituent phases and their interfacial characteristics. Rashad *et al*.[28] conducted a comprehensive comparison of 64 elastic modulus results for concretes using various aggregate types from existing literature and revealed a pronounced influence of aggregate type on the elastic modulus of concrete at different strengths. Specifically, lower stiffness aggregates like sandstone consistently produced concrete with significantly lower elastic modulus across all strength levels.

Due to increased environmental awareness, pozzolan materials have become essential mineral additives for concrete. Primarily composed of silicon dioxide (SiO_2) and aluminum oxide (Al_2O_3),[29] these materials exhibit minimal hydration reactivity on their own. However, in a fine powder state with moisture, they can react with $Ca(OH)_2$ from cement hydration process at room temperature, undergoing a pozzolanic reaction. This reaction forms cementitious compounds such as C-S-H and calcium aluminate hydrate (C-A-H) colloids.[30,31] Therefore, pozzolan materials are considered cementitious and can substitute part of the cement when mixed into concrete.

In concrete, nano-silica (NS) and silica fume (SF) can operate on two distinct levels. The primary level is associated with the chemical impact arising from the pozzolanic reaction between silica and calcium hydroxide ($Ca(OH)_2$) and form the additional calcium silicate hydrate (C-S-H) gel, a pivotal component contributing to the strength and density of the hardened binder paste.[32] The pozzolanic reactivity is notably heightened by the larger surface area of pozzolanic particles, thereby accelerating the rate of the pozzolanic activity.[33] The secondary level pertains to a physical effect due to the significantly smaller size of nano silica compared to cement because of its service properties such as filling the voids, enhancing density, reduction in permeability and lowering the weight of concrete.

In terms of concrete strength, studies have demonstrated that both compressive and flexural strength can increase by up to 75% with the addition of small amounts of NS (0-10%). Shakhmenko *et al*.[34] conducted tests on the mechanical properties of cement paste by replacing cement with varying amounts of SF and NS. Samples were prepared with 2% of cement mass for both cement/SF paste and SF and NS compositions. The results revealed that mixes containing SF and NS particles exhibited higher compressive strength values (more than 3 times higher at early ages and approximately 15% higher at 28 days) and displayed a prolonged hardening effect compared to pure cement paste.[35] These elevated compressive strength values were evident at all stages of hardening, with notable differences observed in the early stages.

The agenda behind incorporating nano-particles into cement-based materials like SCC is to enhance the microstructure of the composite, thereby improving its overall physical, mechanical, and long-term behavior.[36] Cement hydration involves a chemical reaction among water, C_3S, and C_2S, leading to the production of $Ca(OH)_2$ crystals and C-S-H gel.[37] However, $Ca(OH)_2$ crystals, due to their leaching behavior, are undesirable in the cement matrix, unlike C-S-H gel, which is the primary contributor to the strength of cement-based materials. To mitigate the presence of calcium hydroxide crystals in the cement matrix, one approach is to introduce nano-particle materials such as nano-silica to react with the existing $Ca(OH)_2$ crystals. This reaction results in the generation of additional C-S-H gel while reducing the amount

of $Ca(OH)_2$ crystals within the matrix. Consequently, this process enhances the microstructure, mechanical properties, and permeability performance of cement-based materials.[38]

SF consists of spherical particles with an average diameter of 0.1 microns, approximately 100 times smaller than FA particles. Adding SF as a binder enhances the workability of Ultra-High Performance Concrete (UHPC) due to its finer particle size and spherical shape, which effectively fills voids between coarser particles.[39] Beyond its role in particle packing, SF contributes to the strength of UHPC through its pozzolanic activity. Research suggests that using 25% SF with low carbon content (<0.5%) optimally improves UHPC properties. However, the ideal SF content varies significantly depending on the water-to-binder ratio, with lower ratios requiring less SF.[40]

The increasing prominence of sustainability and the imperative to reduce carbon footprints in construction has led to the increased incorporation of mineral additives, such as FA, into concrete. Modern concrete demands high fluidity, early strength, and a low water-cement ratio, criteria through mineral additives. Beyond these benefits, the non-reactive portion of mineral additive acts as micro-aggregates, enhancing the packing effect within the matrix. This advantage opens avenues for achieving higher Young's modulus by strategically manipulating coarse and fine aggregate content in the mix. Similar to conventional concrete, the water-to-cement (w/c) or water-to-binder (w/b) ratio stands out as a crucial factor influencing the compressive strength of SCC at various curing stages. Typically, the w/b ratio in SCC is lower than that in regular concrete. A reduced w/b ratio implies a higher quantity of cement and binder materials in the mix, resulting in elevated compressive strength and a more uniform matrix. In their study, Faraj *et al*.[41] investigated the influence of different w/b ratios on the destructive strength of SCC. They observed a significant improvement in the compressive strength of SCC across all curing ages (3, 7, 28, and 56 days) when the w/b ratio was reduced from 0.45 to 0.35. Furthermore, most researchers[42,43] asserted that the w/b ratio exerts a more pronounced impact on the compressive strength of normal concrete (NC) compared to its influence on the compressive strength of SCC.

However, deploying high volumes of aggregate and large aggregate sizes poses challenges during placement of concrete leading to frictional resistance and potential blockages in concrete pipelines. To address these concerns, the study explores the use of mineral additives as viscosity enhancers and pumping aids, offering a holistic solution to enhance Young's modulus and overcome practical challenges in concrete placement operations. This research aims to contribute valuable insights into the optimization of concrete compositions, striking a balance between material performance, economic considerations, and environmental sustainability. The subsequent sections will delve into the experimental methodologies, results, and discussions, comprehensively examining the intricate interplay between aggregate characteristics, mineral additives utilization, and the enhancement of Young's modulus in high-performance concrete.

This research paper aims to comprehensively investigate and analyze the factors influencing the Young's modulus in concrete with a focus on achieving enhanced performance for specialized applications. The study objectives are to investigate the impact of varying the maximum aggregate size on the compressive strength and Young's modulus of concrete, while assessing the influence of mineral additives. Furthermore, the study examined the mechanical strength of concretes through split tensile, compressive, and flexure strength tests, following aggregate petrographic and concrete morphological studies.

2. Experimental methodology

2.1 Materials

In this study, ordinary Portland cement of grade 43 (OPC 43), adhering to the specifications outlined in bureau of Indian standards (IS 269: 2015),[44] was used as binder. The mineralogical compositions of this cement were C_3S (55.26%), C_2S (28.12%), and a cumulative sum of C_3A and C_4AF (16.62 %). Additionally, the concentrations of K_2O and Na_2O are maintained below 0.6%. the cement exhibits distinctive properties, including a heat of hydration below 250 J/g at 7 days and an upper strength limit restricted to 58 MPa. To ensure conformity to these specifications, various physical tests and chemical analyses were conducted on the cement, in accordance with the guidelines provided in IS 269: 2015.[44] The results of these analysis are comprehensively presented in Table 1, providing data essential for the understanding and interpretation of the cement's characteristics.

Table 1. Properties of OPC 43.

Physical properties		Chemical properties (wt%)	
Consistency (%)	26	C_3A	4.17
Initial setting time (min)	140	C_3S	55.26
Final setting time (min)	230	C_2S	28.12
Compressive strength (MPa)		C_4AF	12.45
3 days	34	Insoluble residue (wt%)	0.44
7 days	44.5	Magnesia (wt%)	1.61
28 days	55.48	Sulphuric anhydride (wt%)	2.52
Soundness;		Loss of ignition (wt%)	1.99
Le Chatelier's method (mm)	1.67	Total alkali content (wt%)	0.43
Auto clave method (%)	0.037	Chloride content (wt%)	0.014
Specific surface (m^2/kg)	293	Heat of hydration at 7 days J/g	234
		Al_2O_3/Fe_2O_3	0.94

Aggregates were used in two types to contribute to the properties of the concrete. The primary aggregate utilized was charnockite (metamorphic aggregate), processed through a multi-stage crushing procedure involving a jaw crusher, cone crusher, and vertical shaft impactor. The resulting cubical-shaped aggregates are complemented by completely crushed sand, obtained through a dry air classifier that separates particles below 75 µm. Rigorous testing assesses the physical, chemical, and mechanical properties. Additionally, hematite, a meta-sedimentary rock, serves as a secondary aggregate specifically chosen for its role in producing heavy density concrete (HDC). High density aggregates (HDA) are derived from crushed hematite iron ore, ensuring specific gravity exceeding 4.65 and iron content more than 60%. The meticulous processing of both charnockite and hematite aggregates underscores the comprehensive approach taken in this research. The physico chemical properties are represented in Table 2. The grading of all aggregates is represented in Fig. 1, conforming to the standards outlined in IS 2386 Part 1:2019.[45]

To enhance the elasto-mechanical properties of HPC, the sources and purity of the mineral additives were discussed to maintain the consistency of the concrete mix. To ensure the stability of experimental conditions, the mineral additives were tested in climate control laboratory by maintaining a consistent temperature of 27 °C ± 2 °C and targeted humidity level of 50% ± 5%. FA with low calcium content was used as a primary mineral additive procured from Ukai Thermal Power Station, Gujrat, India. The material conformed to IS 3812 part 1: 2013.[46] to ensure compliance with industry norms. The FA was carefully characterized with a Loss on ignition (LOI) limited to 2% and particles retained on a 45-micron sieve capped at 20%. Integrated at a 40% replacement by weight of cement for M45 grade concrete, the research systematically examined and presented the impact of FA on the hardened properties at 7 and 28 days. The purity of mineral additive is represented in Table 3. SF was sourced as secondary mineral additive from Elkem Ltd., Mumbai, India. The densified SF was used at replacement levels of 10% and 8% for M 60/20 grade concrete conforming to IS 15388:2003[47] standards. Renowned for its fine particle size and high reactivity, SF influence on the hardened properties of the concrete was rigorously investigated and reported in Table 4.

2.2 Test methods

In this research, three essential raw materials, namely aggregate, cement, and admixture, were meticulously selected to formulate a total of 14 concrete mixes. The investigation commenced with a series of fundamental tests conducted on

Table 2. Properties of charnockite and hematite aggregate.

Parameters	Charnockite	Hematite
Petrography for strained quartz (%)	2%	-
Soundness test by sodium sulphate (%)	0.52	0.18
Rock crushing strength (MPa)	84.33	135.44
Chloride content (%)	0.004	0.009
Sulphate content (%)	0.034	0.082
Specific gravity	2.73	4.7
Water absorption (%)	0.84	0.35
Flakiness index (%)	9.24	8.55
Elongation index (%)	10.96	10.24
Crushing value (%)	23.81	11.21
Impact value (%)	22.63	11.09
Abrasion value (%)	21.09	18.53

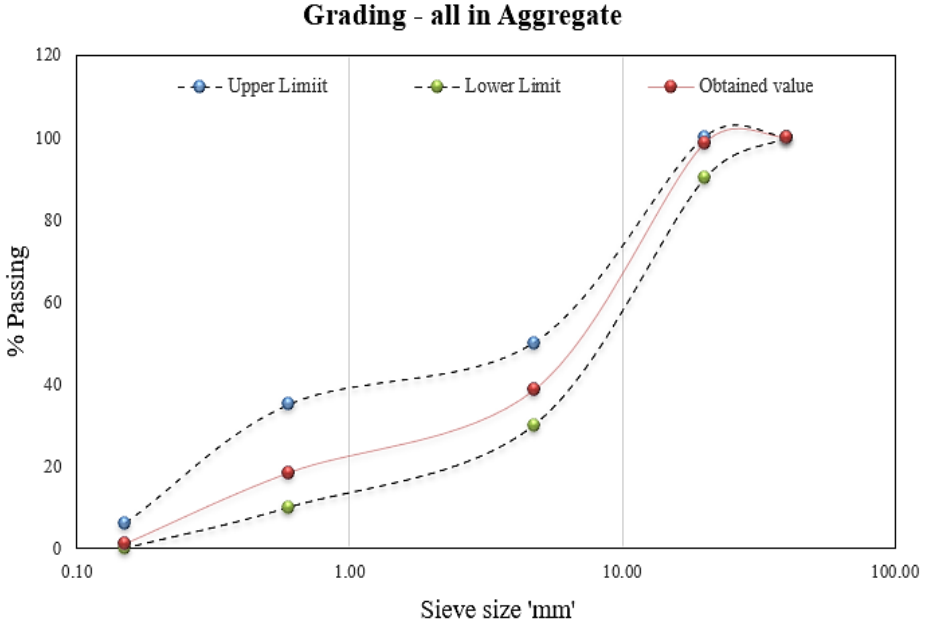

Fig. 1 Grading of all in aggregate as per IS 2386-part 1:2019 specification.

Table 3. Properties of FA.

Physical properties		Chemical properties	Wt%
Fineness-specific area (m^2/kg)	396	SiO_2	56.3
Particles retained on 45 μm IS sieve (%)	12.21	Al_2O_3	22.4
Lime reactivity (%)	4.67	Fe_2O_3	12.6
Compressive strength of plain mortar cubes		MgO	0.6
(MPa);		SO_3	2.4
7 days	82.03	CaO	4.13
28 days	93.22	Cl^-	0.022
Soundness (%)	0.036	LOI, 1 h	1.55

Table 4. Properties of SF.

Physical properties		Chemical properties	Wt%
Specific gravity	2.13	SiO_2	87.29
Particles retained on 45 μm IS sieve (%)	-	Na_2O	1.65
Compressive strength of plain mortar cubes (MPa); 7 days	109	Moisture content	3.12
Specific surface area (m^2/g)	21.3	LOI, 1 h	0.67

the raw materials, encompassing tests to assess their individual characteristics. Subsequently, concrete mixes were meticulously prepared using the specified raw materials. The basic properties of the raw materials and the freshly prepared concrete mixes were examined. For a comprehensive evaluation of the concrete mixes, a series of tests, including split tensile, compressive, flexural, and scanning electron microscopy (SEM) tests, were conducted. The detailed experimental procedures, including raw material testing and concrete mix preparation, are elucidated in the flow diagram presented Fig. 2.

2.2.1 Concrete mix design

To analyze the Young's modulus values, trial mixes were categorized into two groups: NC and mineral admixture concrete (MAC). The trial studies involved metamorphic and hematite aggregates (Meta sedimentary) for the production of 14 mixes, catering to both normal weight and heavy concrete. The experiments were conducted in the laboratory, and samples were cast to ascertain fresh and hardened concrete properties based on the required mix design as per IS 10262:2019.[48] A meticulous schedule for sample casting and trial mix observations was maintained prior to each trial. In the

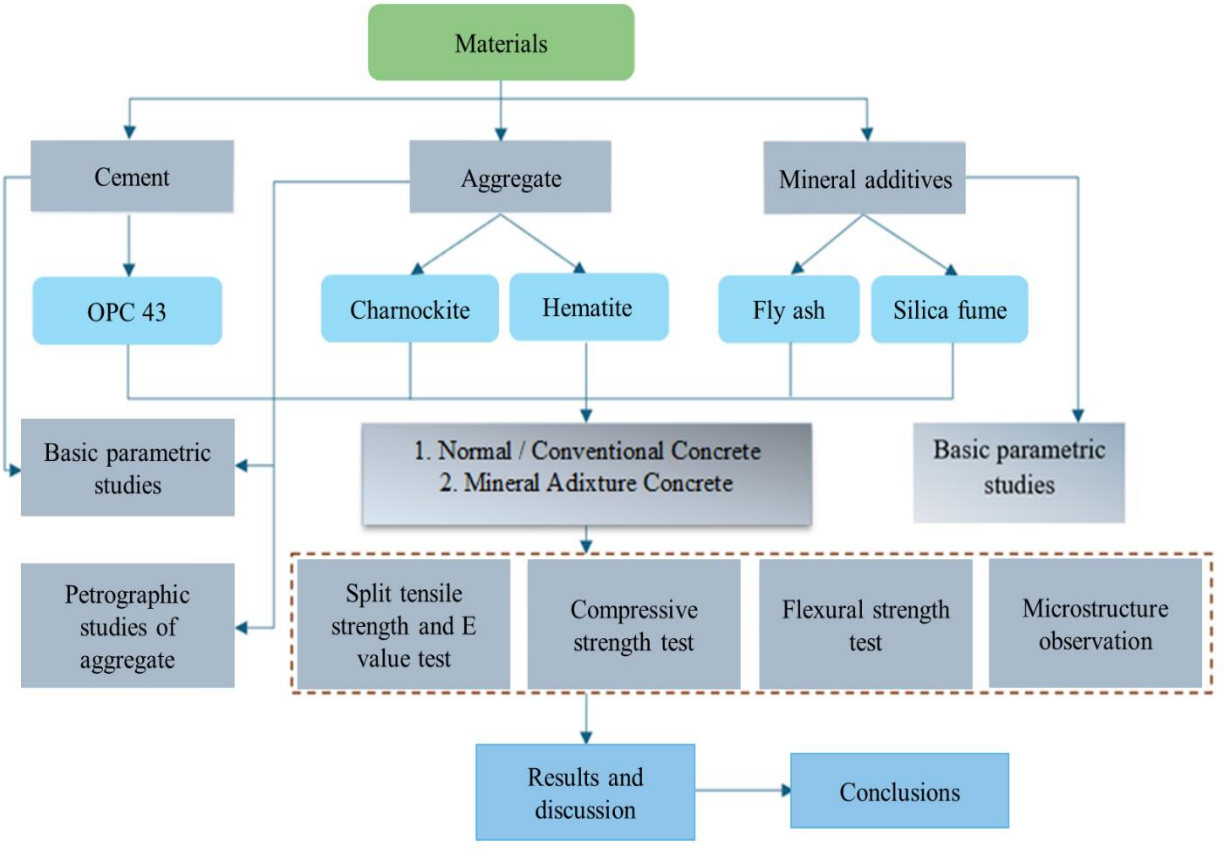

Fig. 2 Flowchart representing methodology of the study.

conventional concrete, the trial mixes were designed for three NC grades, namely M 35/40, M 35/20, and M 50/20, each with different percentages of coarse aggregates and cement content (M Stands for Mix, 35 & 50 are the 28 days compressive strength in MPa and 20 is the maximum size of aggregate). Based on the analysis of fresh and hardened properties, some data was modified. For instance, the M-1 mix of M 35/40 grade was proportioned with 58% coarse aggregate and 330 kg cement content. Subsequent mixes (M-2 to M-6) involved adjustments in coarse aggregate and cement content to optimize properties. H-1 represented HDC for H35 grade, designed using hematite aggregate with specific gravity exceeding 4.65 and iron content surpassing 60% and mix of concrete was given in Table 5.

The other type of concrete is MAC. In this mix design synthesis, the mineral additives such as FA and SF were incorporated into mixes M-8 to M-11 and H-2, H-3 (H30, H35, M45, and M60 grades of concrete) at varying supplementary cementitious replacement levels. The mix design compiles with natural aggregates (metamorphic and hematite), and other ingredients as detailed in Table 6. The use of mineral additives acted as a pumping aid and viscosity enhancer, enhancing concrete pumping properties over desired horizontal and vertical distances. Moreover, the inclusion of mineral additives allowed for a reduction in water-to-cement ratio, and the need for fine aggregate was significantly decreased due to the high fineness and maximum surface area of SF and FA.

The detailed analysis of conventional and mineral admixture concrete mixes provides valuable insights into the optimization of Young's modulus value, showcasing the influence of aggregate type and mineral additives on the fresh and hardened properties of concrete. These findings contribute to the enhancement of concrete mix designs to improve the structural performance.

2.2.2 Petrographic study of the aggregate

Petrographic studies of aggregates play a pivotal role in assessing the quality and characteristics of construction materials, particularly in concrete research.[49] This research utilized a Nikon polarizing microscope (model no. JVD1288R) from Japan to analyze the petrography of aggregates. The procedure for conducting petrographic studies typically involves collecting representative samples of aggregates used in concrete, followed by the preparation of thin sections. These thin sections are then examined under a polarizing microscope to analyze the mineral composition, texture, and petrographic features of the aggregates.[50] The identification of minerals, potential deleterious substances, and the overall rock texture aids in understanding the potential effects on concrete performance, durability, and potential reactions with cementitious materials. Petrographic studies contribute

Table 5. Mix design for NC.

Mix compositions	M-1	M-2	M-3	M-4	M-5	M-6	H-1
Grade	M 35/40	M 35/40	M 35/20	M 35/20	M 50/20	M 50/20	H 35/20
Max. size of aggregate (mm)	40	40	20	20	20	20	20
Cement (kg/m^3)	330	340	390	375	450	450	385
Water (kg/m^3)	145	146	156	156	144	144	161
Coarse aggregate (kg/m^3);							
40 mm size	512	530	-	-	-	-	-
20 mm size	405	434	745	769	776	796	1109
10 mm size	320	328	429	423	427	447	941
Fine aggregate (kg/m^3)	896	826	817	796	738	777	1310
Admixture (kg/m^3)	2.64	2.72	3.12	3.00	3.38	4.05	3.85

Table 6. Mix design for MAC.

Mix compositions	M-8	M-9	M-10	M-11	H-2	H-3
Grade	M 45/20	M 45/20	M 60/20	M 60/20	H 30/20	H 35/20
Max. size of aggregate (mm)	20	20	20	20	20	20
Cement (kg/m^3)	288	300	450	450	370	334
SF (kg/m^3)	-	-	45	35	-	16
FA (kg/m^3)	192	200	-	-	60	-
Water (kg/m^3)	145	145	144	146	163	151
Coarse aggregate (kg/m^3);						
20 mm size	692	703	736	813	822	724
10 mm size	449	444	490	445	829	790
Fine aggregate (kg/m^3)	729	704	660	667	1501	1178
Admixture (kg/m^3)	6.72	7.00	2.97	4.37	3.22	5.25

valuable information for optimizing concrete mix designs, ensuring compatibility between aggregates and cementitious materials, and enhancing the long-term durability and performance of concrete structures.[51]

2.2.3 Split tensile strength test

Split tensile strength is a crucial parameter in assessing the durability and performance of concrete structures.[52] It measures the tensile strength of concrete by subjecting cylindrical specimens to diametral loading in HEICO based Compressive Testing Machine of capacity 3000 kN with rate of loading of 1.62 kN/s to 2.43 kN/s. The procedure involves casting standard cylindrical specimens with a diameter-to-height ratio of 1:2 and allowing them to cure under standard conditions. Subsequently, the specimens were placed in a testing machine with diametral loading platens. The test set up of split tensile strength is shown in Fig. S1. A diametral load is applied at a constant rate until failure occurs along the plane perpendicular to the applied load.[53] The split tensile strength can be calculated from the following equation 1.

$$f_t = \frac{2P}{\pi dl} \quad (1)$$

where,

f_t = Split tensile strength (MPa)

P = Maximum load (N)

d = Diameter of specimen (mm)

l = Length of specimen (mm)

This parameter provides valuable insights into the ability of concrete to resist tensile stress, which is particularly essential in structures exposed to varying environmental conditions and loading scenarios.[54]

2.2.4 Flexural strength test

Flexural strength, also known as modulus of rupture (MOR), is a critical parameter in evaluating the ability of concrete to withstand bending stresses.[55] The procedure for determining flexural strength involved casting standard rectangular prismatic specimens with specified dimensions (150 mm × 150 mm × 750 mm) following the curing at standard ambient temperature. Further, the cured specimens were placed in a flexural testing machine of capacity 100 kN with a rate of loading of 4 kN/min with four-point loading with the gradual load application until the specimen failed in flexure.[56] The flexural strength can be calculated from the following equation 2.[57]

$$\sigma = \frac{Pl}{bd^2} \quad (2)$$

where,

σ = Flexural strength (MPa)

P = Maximum load (N)

l = Span between supports (mm)

b = Width of specimen (mm)

d = Depth of specimen (mm)

This parameter is fundamental in assessing the structural performance of concrete elements, such as beams and slabs, providing valuable information for design and construction practices to ensure the integrity and safety of concrete structures.[58]

2.2.5 Compressive strength test

Compressive strength is a fundamental parameter in evaluating the mechanical performance of concrete, commonly measured through cube and cylinder specimens.[59] In a research paper, the procedure for determining compressive strength typically involves casting standard cube (150 mm × 150 mm × 150 mm) and cylindrical (150 mm in diameter and 300 mm in height) specimens, subjecting them to standard curing conditions. The specimens were then tested in an Associated Instruments Manufacturers India (Pvt.) Ltd. (AIMIL) based compression testing machine of capacity 2000 kN with rate of loading of 5.2 kN/s for cubes and 4 kN/s for cylinders, by applying a gradually increasing axial load until failure occurs. The compressive strength can be calculated from the following equation. 3,

$$f_{ck} = \frac{P}{A} \quad (3)$$

where,

f_{ck} = Compressive strength (MPa)

P = Load (kN)

A = Area of specimen (mm^2)

This parameter is pivotal in assessing the concrete's ability to withstand axial loads and is crucial for structural design and quality control in construction projects.

2.2.6 Young's modulus test

The Young's modulus (E value) or modulus of elasticity is a critical parameter in characterizing the stiffness and elastic behavior of concrete. Stiffness is a paramount consideration in structural design, particularly in applications where minimal deflection is imperative. The Young's modulus is a significant indicator to measure the material stiffness and represents the stress required to induce unit strain. The procedure for determining Young's modulus of concretes typically involved casting cylindrical specimens and subjecting them to AIMIL based compression testing machine with capacity of 2000 kN with the rate of 4 kN/s to obtain the concrete's initial tangent modulus (Fig. S2). Additionally, direct tensile tests can be conducted to calculate the secant modulus. The Young's modulus is then computed by dividing stress by strain within the elastic deformation range. A higher Young's modulus indicates greater stiffness and rigidity in the material, suggesting better load-bearing capacity and less deformation under stress. Conversely, a lower Young's modulus signifies a more flexible and ductile material with higher deformability. Understanding the Young's modulus of concrete is crucial in structural engineering, aiding in the design of resilient and efficient structures based on the material's elastic properties.

2.2.7 Morphological studies

To analyze the morphology of all concrete samples, the representative sections of the structure should be selected

carefully by ensuring that they are adequately cured.[60] The microstructure analysis was depicted using a TESCAN-VEGA3 LMU electron microscope at an accelerating voltage of 10 kV.

3. Results and discussions

3.1 Petrographic study of aggregate

The petrographic study conducted on two distinct types of aggregates, namely metamorphic rock samples classified as charnockite and hematite aggregate, provided comprehensive insights into their mineralogical compositions and textural characteristics. The metamorphic rock displayed a coarse-grained, inequigranular structure, with a predominant composition of quartz, plagioclase feldspar, hypersthene, biotite, magnetite, ilmenite, zircon, and apatite. Microscopic observations revealed that quartz and plagioclase feldspar were the dominant minerals, exhibiting anhedral and subhedral forms, respectively. Hypersthene appeared colorless to pinkish, displaying strong pleochroism, while biotite exhibited a flaky habit with well-developed cleavage, similar results were reported by Beyene *et al*.[49] The granulose texture and the presence of ant perthite development, along with observable features like bending and tapering of lamellae, indicated the classification of the rock as charnockite. This classification aligns with the granulite group and designates it under the trade group of metamorphic rocks as per IS 383:2016.[61] The hematite aggregate exhibited a distinctive composition, with iron oxide and quartz as major constituents. Accessory minerals included calcite, orthoclase-feldspar, and muscovite. Microscopic analysis revealed the uniform distribution of subhedral and anhedral iron oxide grains, with some euhedral grains observed. Quartz grains, ranging from 110 µm to 180 µm, exhibited sharp grain margins and a well-graded distribution. Calcite grains, subhedral orthoclase grains, and needle-shaped muscovite grains were also present, contributing to the overall heterogeneity of the aggregate. The strained quartz was negligible, and undulatory extinction angle varied between 140 and 160. The classification of the hematite aggregate as a meta-sedimentary rock within the trade group specified by IS 383:2016 was attributed to the observed mineralogical composition and associated features. These petrographic studies, presented in Fig. 3, provide a detailed understanding of the diverse mineralogical compositions and textures of the studied aggregates. Such knowledge is crucial for optimizing concrete mix designs tailored to the specific characteristics of these aggregates, ensuring the durability and long-term performance of concrete structures in construction applications.

3.2 Split tensile strength test

In concrete, the split tensile strength is a vital indicator of its ability to withstand tensile stresses. Higher split tensile strength values generally indicate superior resistance to cracking and improved durability. In the context of this study, the progressive increase in tensile strength observed in conventional concrete mixes with higher grades suggests a positive correlation between concrete grade and tensile strength. In MAC mixes, the incorporation of mineral additives led to further enhancements, highlighting the advantageous impact of these additives on concrete's mechanical properties. The superior split tensile strength values observed in hematite aggregate-containing mixes underscore the potential for formulating high-strength, heavy-density concrete. In the conventional concrete mixes, the split tensile strength demonstrated a discernible trend across different grades with an average of three specimens in each mix. Figs. 4 and 5 show results of split tensile strength for NC and MAC.

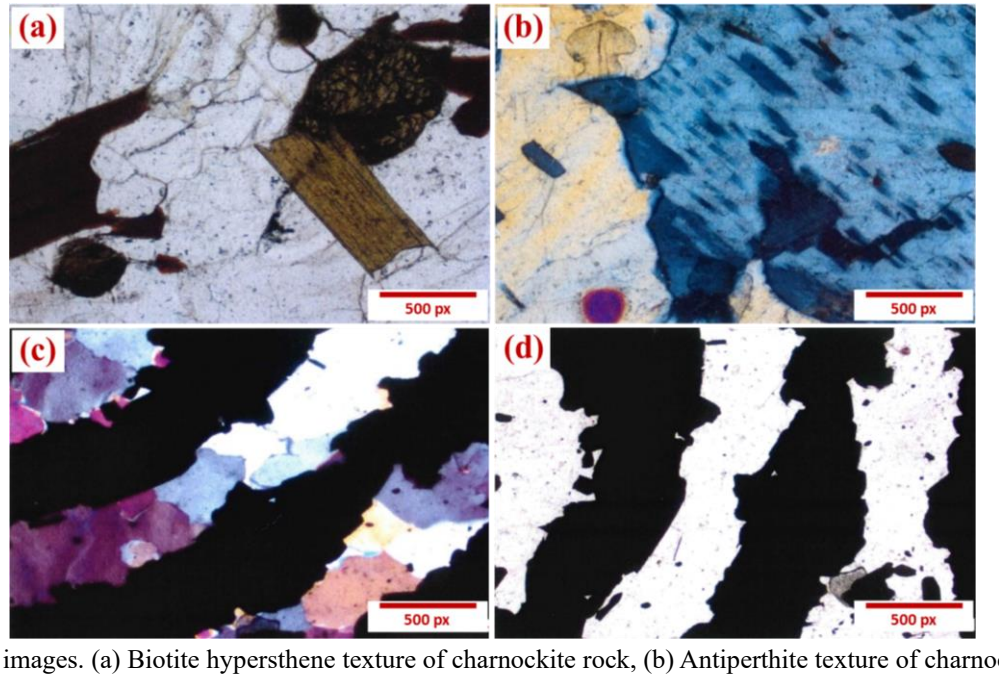

Fig. 3 Petrographic images. (a) Biotite hypersthene texture of charnockite rock, (b) Antiperthite texture of charnockite rock, (c) Banded rock with quartz-hematite and (d) Iron oxide and quartz layer in hematite rock.

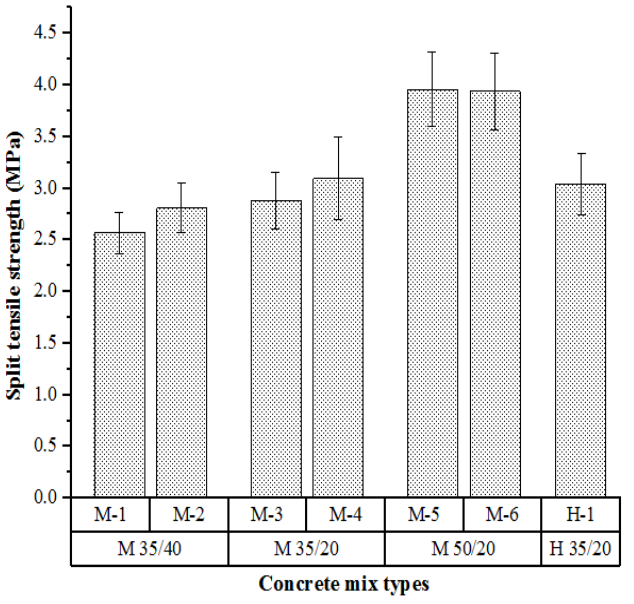

Fig. 4 Split tensile strength of NC concretes.

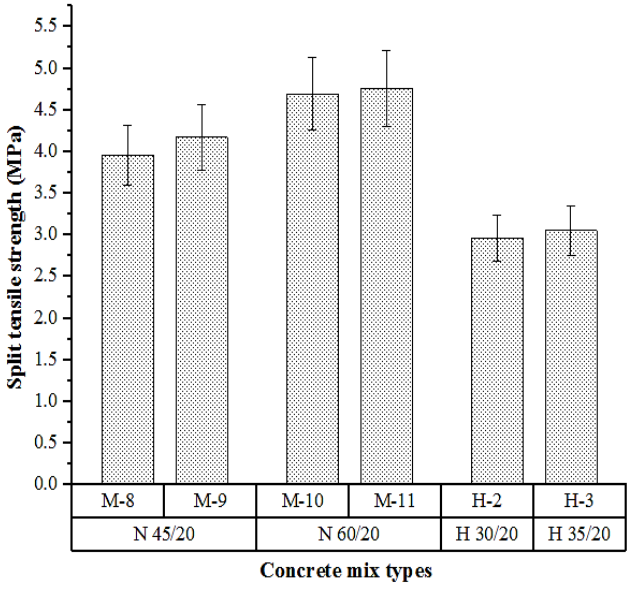

Fig. 5 Split tensile strength of MAC concretes.

For the M 35/40 mixes (M-1 and M-2), the values stood at 2.57 MPa and 2.81 MPa, respectively. A modest increment was observed in the M 35/20 mixes (M-3 and M-4), recording 2.88 MPa and 3.1 MPa, signifying a tangible improvement in tensile strength with a higher cement-to-aggregate ratio. The M 50/20 mixes (M-5 and M-6) exhibited further enhancement, achieving 3.96 MPa and 3.94 MPa, reflecting the impact of elevated concrete grade on tensile strength. The H-1 mix (H 35/20) showcased a split tensile strength of 3.04 MPa, underscoring the suitability of hematite aggregates in formulating heavy-density concrete. The split tensile strength results for MAC mixes (M-8 to H-3) demonstrated the influence of mineral additives on mechanical performance. In the N 45/20 mixes (M-8 and M-9), split tensile strength ranged from 2.96 MPa to 3.05 MPa, illustrating a positive effect due to the inclusion of FA. The N 60/20 mixes (M-10 and M-11) showed further improvement, reaching 3.95 MPa and 4.17 MPa, indicating enhanced tensile strength attributed to the use of SF. In the H 30/20 and H 35/20 mixes (H-2 and H-3), employing hematite aggregates, the split tensile strength surpassed 4.7 MPa, emphasizing the synergistic effect of mineral additives and hematite aggregates on tensile strength. The results provide valuable scientific insights into the factors influencing split tensile strength, aiding in the formulation of concrete mixes tailored for optimal performance in construction applications.

3.3 Flexural strength test

The flexural strength test results for NC & MAC mixes, incorporating metamorphic and hematite aggregates are presented and discussed below, emphasizing the scientific implications of the observed values. Figs. 6 and 7 show results of flexural strength for NC and MAC, respectively. Flexural strength is crucial in assessing a material's ability to withstand bending stresses. Higher flexural strength values typically indicate superior resistance to bending and cracking.

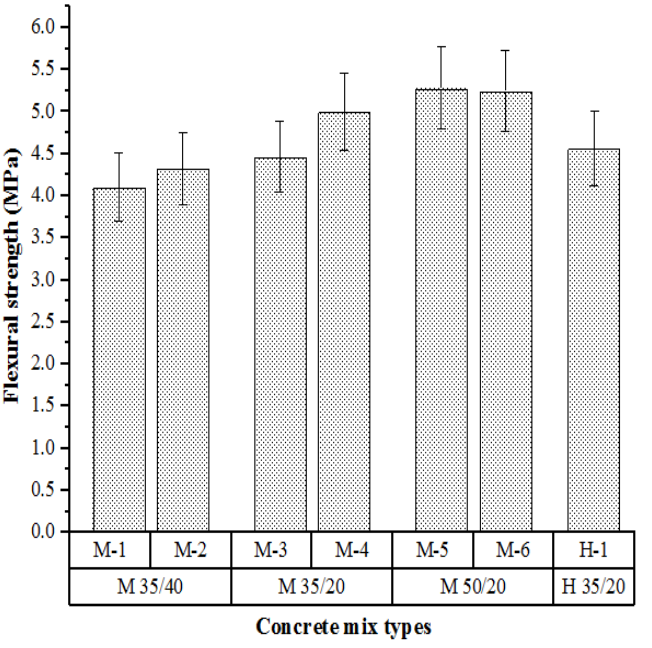

Fig. 6 Flexural strength of NC concretes.

In the NC mixes, the flexural strength exhibited variations across different grades with an average of three specimens in each mix. For the M 35/40 mixes (M-1 and M-2), the values were recorded at 4.1 MPa and 4.32 MPa, respectively. A moderate increase was observed in the M 35/20 mixes (M-3 and M-4), reaching 4.46 MPa and 5 MPa, indicating a tangible improvement in flexural strength with a higher cement-to-aggregate ratio. The M 50/20 mixes (M-5 and M-6) showed further enhancement, achieving 5.28 MPa and 5.24 MPa, reflecting the impact of elevated concrete grade on flexural strength. The H-1 mix (H 35/20) exhibited a flexural strength of 4.56 MPa, emphasizing the potential of hematite aggregates in heavy-density concrete.

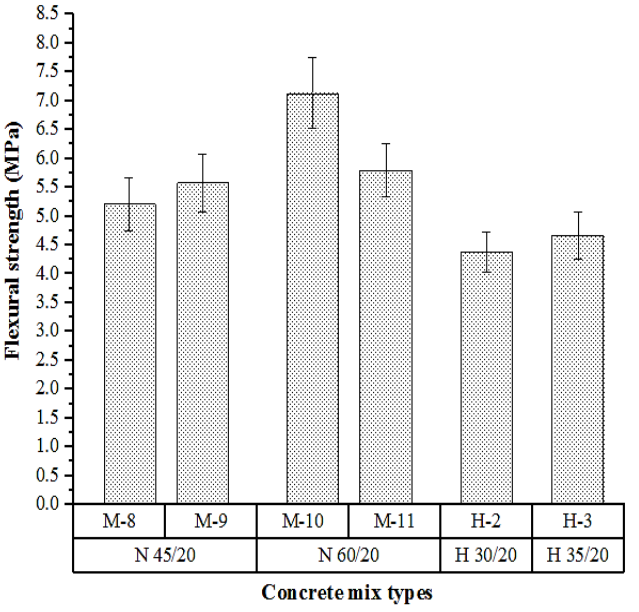

Fig. 7 Flexural strength of MAC concretes.

The flexural strength results for MAC mixes (M-8 to H-3) demonstrated the influence of mineral additives on mechanical performance. In the N 45/20 mixes (M-8 and M-9), flexural strength ranged from 4.38 MPa to 4.67 MPa, illustrating a positive effect due to the inclusion of FA. The N 60/20 mixes (M-10 and M-11) showed further improvement, reaching 5.21 MPa and 5.58 MPa, indicating enhanced flexural strength attributed to the use of SF. In the H 30/20 and H 35/20 mixes (H-2 and H-3), employing hematite aggregates, the flexural strength surpassed 7.14 MPa and 5.8 MPa, respectively, emphasizing the synergistic effect of mineral additives and hematite aggregates on flexural strength. The results provide valuable scientific insights into the factors influencing flexural strength, contributing to the formulation of concrete mixes tailored for optimal performance in construction applications.

3.4 Compressive strength of concrete

The compressive strength and cylinder/cubic compressive strength ratio (CSR) of NC mixes (M-1 to M-6 and H-1) are shown in Figs. 8 and 9, respectively, the cylinder compressive strength values ranged from 32.1 MPa to 51.97 MPa, while cube compressive strength values ranged from 42.65 MPa to 64.27 MPa. The M 50/20 mixes (M-5 and M-6) exhibited the highest strength, aligning with the higher concrete grade. The observed CSR, ranging from 0.75 to 0.81, indicates a reasonably consistent relationship between cylinder and cube compressive strengths in NC.

For MAC mixes (M-8 to H-3), the cylinder compressive strength values ranged from 38.46 MPa to 62.05 MPa, while cube compressive strength values ranged from 50.48 MPa to 76.96 MPa. Notably, the H-3 mix exhibited the highest comprehensive strength, showcasing the influence of hematite aggregates. The observed CSR, ranging from 0.75 to 0.82, suggests a consistent relationship between cylinder and cube compressive strengths in MAC mixes, similar to NC. Fig. 10 and Fig. 11 show results of compressive strength and CSR for MAC, respectively.

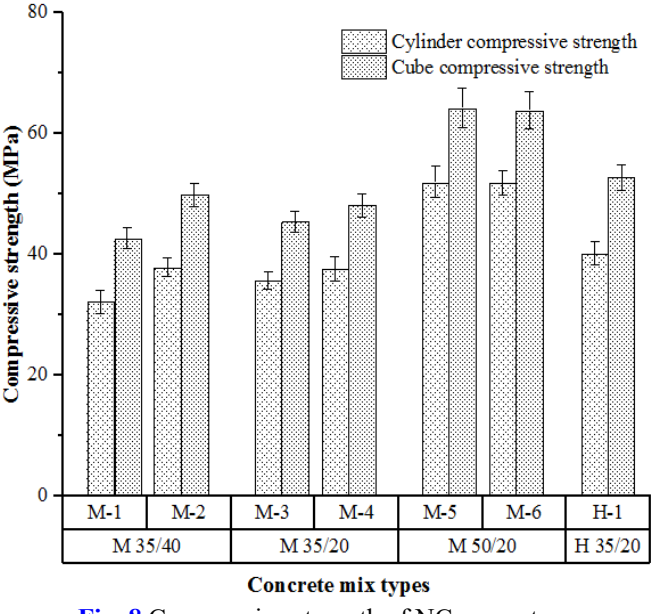

Fig. 8 Compressive strength of NC concretes.

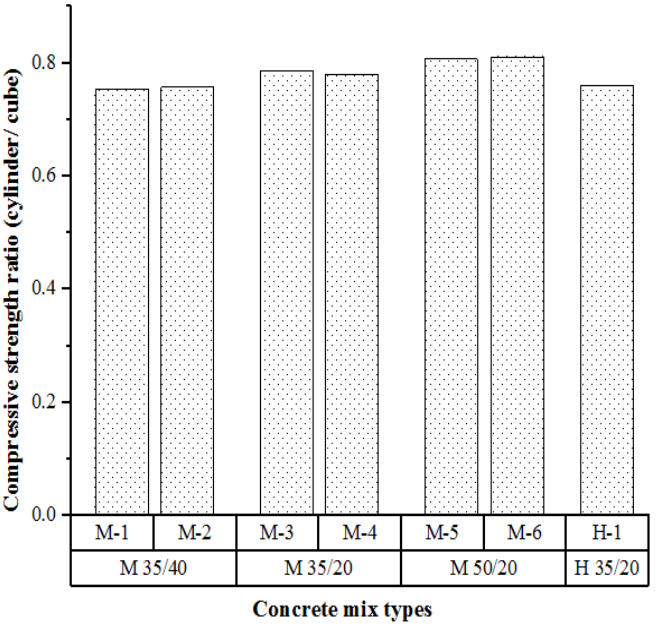

Fig. 9 CSR of NC concretes.

The comprehensive analysis of cylinder and cube compressive strengths provides valuable insights into the mechanical performance of the concrete mixes. The CSR, ranging from 0.75 to 0.82, indicates a relatively stable relationship between the two strength parameters. A higher CSR implies that the cylinder's compressive strength is approaching the cube compressive strength. In both NC mixes and MAC mixes, the observed ratios suggest a consistent trend, highlighting the reliability of both cylinder and cube compressive strength measurements. The variations in the ratios across different mixes can be attributed to factors such as the type of aggregate, concrete grade, and the inclusion of

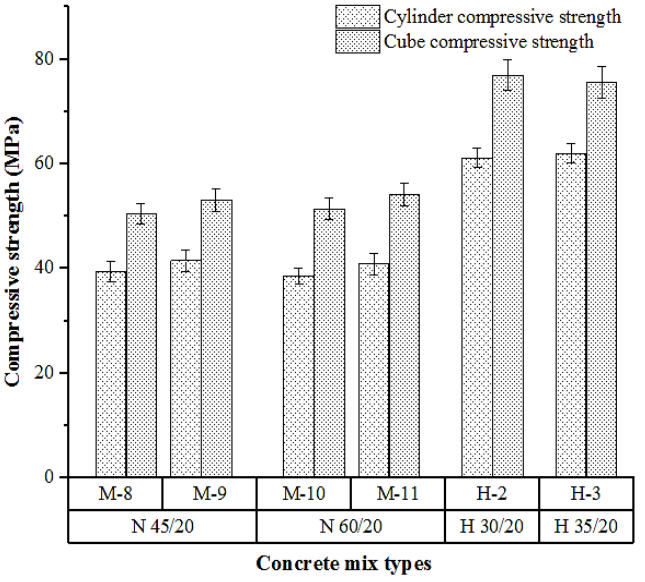

Fig. 10 Compressive strength of MAC concretes.

mineral additives. Notably, the H-3 mix in MAC demonstrated the highest ratio, indicating superior comprehensive strength, possibly due to the synergistic effects of hematite aggregates and mineral additives. The comprehensive strength analysis, as indicated by the CSR, offers valuable insights into the overall mechanical performance of the concrete mixes. These findings contribute to the optimization of concrete mix designs for enhanced strength and durability in construction applications.

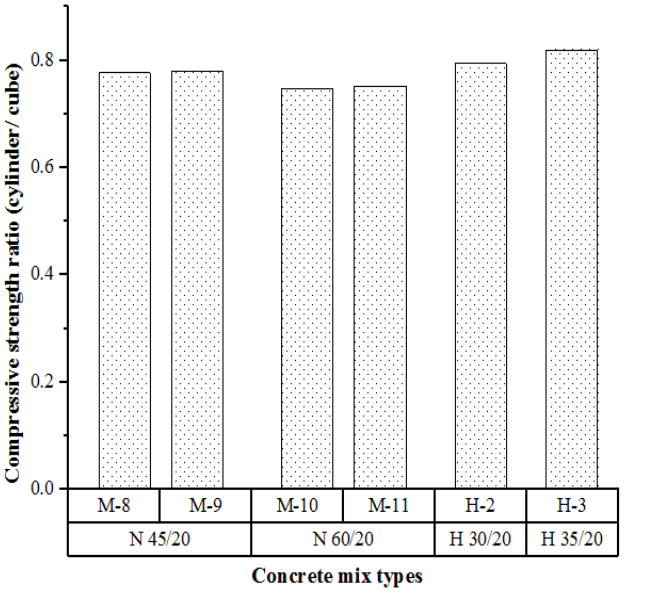

Fig. 11 CSR of MAC concretes.

3.5 Young's modulus of concretes

For conventional concrete mixes (M-1 to M-6 and H-1), Young's modulus values ranged from 32.05 GPa to 40.16 GPa. The M-5 and M-6 mixes, both belonging to the M 50/20 grade, exhibited the highest Young's modulus values. The observed trend suggests an increase in Young's modulus with higher concrete grades, indicating the material's improved stiffness and resistance to deformation. The H1 mix, incorporating hematite aggregates, also showed a relatively high Young's modulus value, emphasizing the potential of hematite aggregates in enhancing concrete stiffness. Figs. 12 and 13 show the result of Young's modulus value for NC and MAC, respectively.

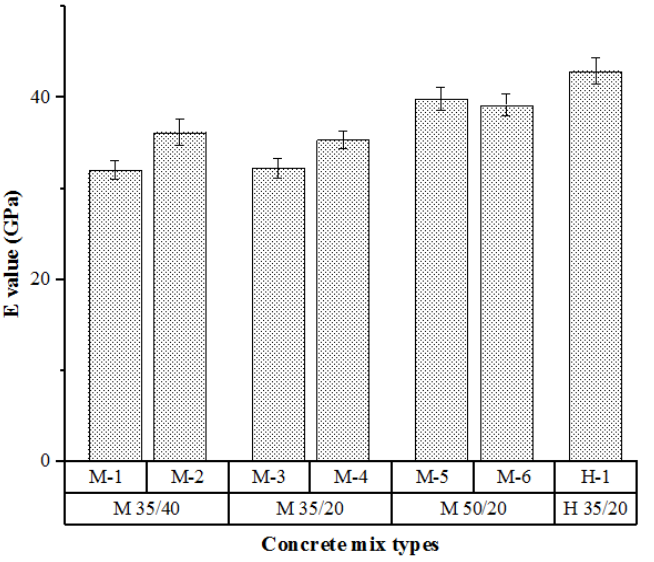

Fig. 12 Young's modulus of NC concretes.

For MAC mixes (M-8 to H-3), Young's modulus values ranged from 35.67 GPa to 42.42 GPa. The H-2 mix demonstrated the highest Young's modulus value, followed closely by H-3. These high values suggest that the combination of mineral additives and hematite aggregates contributes to superior stiffness in MAC. The observed trend also indicates that the incorporation of mineral additives can influence Young's modulus positively.

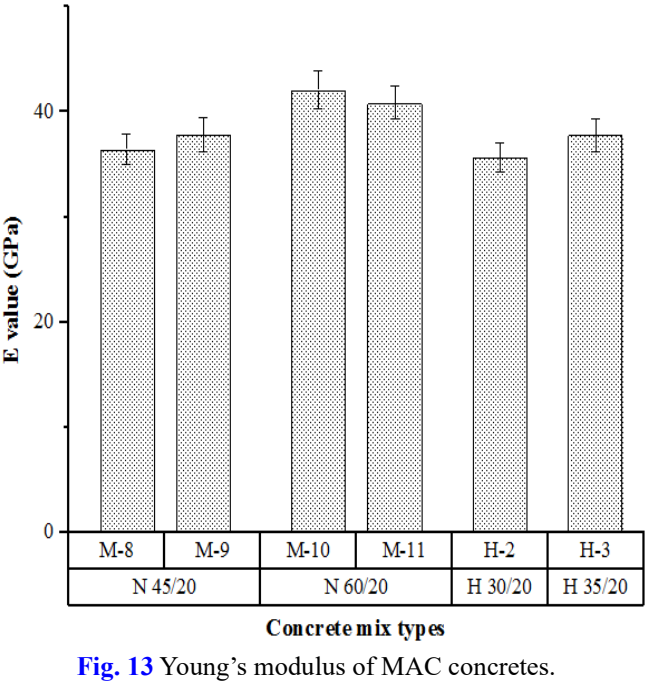

Fig. 13 Young's modulus of MAC concretes.

The statistical analysis of Young's modulus was conducted using test results from 40 cylindrical samples for each concrete mix, resulting in a total of 320 data points across eight different concrete mixes for both NC and MAC, as outlined in Table 7. The coefficient of variance (Cof.V) was calculated using the average and standard deviation of the samples, employing the data analysis tool in MS Excel. Among the mixes, NC M 35/20 exhibited the lowest mean Young's modulus at 35.77 GPa, while MAC N 60/20 showed the highest Young's modulus of 42.42 GPa. The overall mean Young's modulus across all samples was found to be 38.70 GPa, with an average standard deviation of 1.86 GPa. The mix NC M 35/40 had the greatest variability, indicated by a Cof.V of 0.0498, whereas the MAC N 60/20 mix had the least variability, with a Cof.V of 0.0429. The overall dataset produced a Cof.V of 0.048, which is slightly below 5%, suggesting a statistically significant finding of Young's modulus.

The study provides valuable insights into the influence of aggregate type, concrete grade, and mineral additives on Young's modulus. These findings contribute to the optimization of concrete mix designs for improved structural performance and stiffness in various construction applications.

3.6 Morphology of concretes

The SEM morphology study was conducted on all concrete mixes after 28 days to elucidate the microstructural characteristics at the accelerating voltage of 10 kV. SEM analyses at varying magnifications were employed to examine the intricate details of each concrete mix. The investigation revealed distinct microstructural features for different mixes as shown in Fig. 14. In the M 35/20 mix, SEM images indicated the formation of C-S-H gel, with the development of small, sharp needle-like structures. This observation suggests

Table 7. Statistical analysis of Young's modulus.

Concrete Mixes	No. of samples	'E' value Mean (GPa)	'E' Value Median (GPa)	St. Dev (GPa)	Cof.V (T<=t)
NC M 35/40	40	36.71	36.31	1.93	0.0498
NC M 35/20	40	35.77	35.82	1.76	0.0492
NC M 50/20	40	40.16	40.27	1.94	0.0483
NC H 35/20	40	41.75	41.76	2.1	0.0489
MAC N 45/20	40	37.86	37.74	1.76	0.0465
MAC N 60/20	40	42.42	42.44	1.82	0.0429
MAC H 30/20	40	37.95	37.44	1.78	0.0469
MAC H 35/20	40	36.55	36.38	1.82	0.0491
Average of all Mixes	320	38.70	38.52	1.86	0.048

T-obtained value, t – standardised P value (0.05)

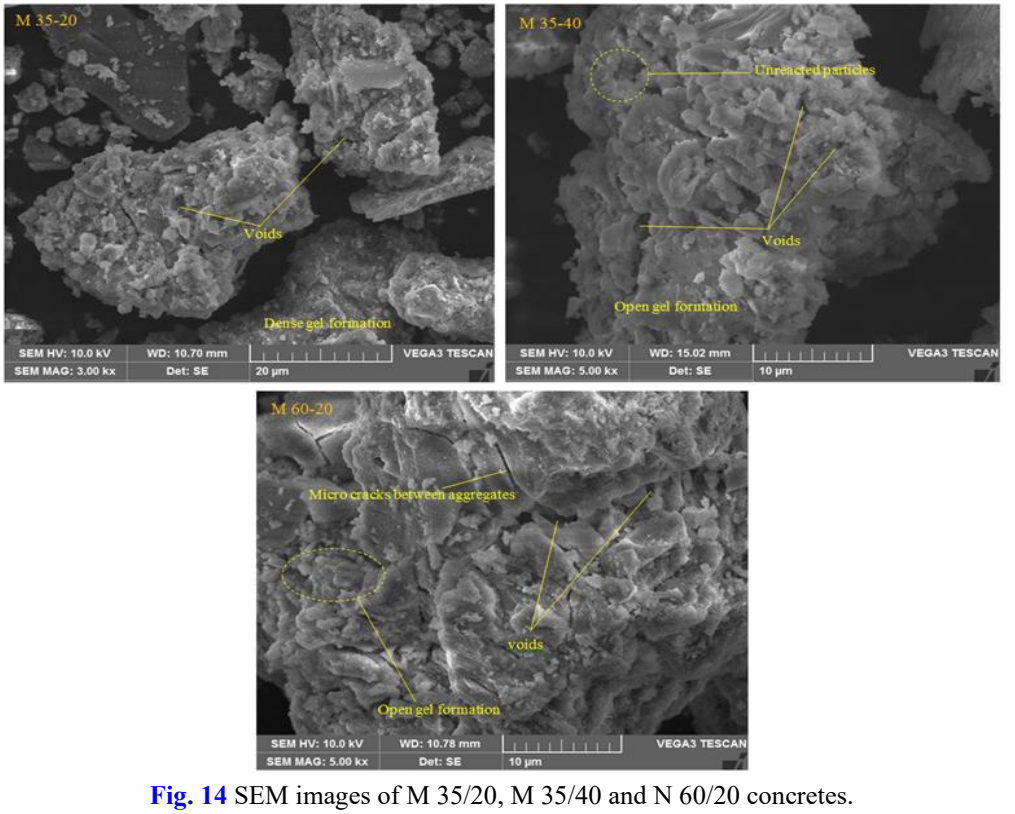

Fig. 14 SEM images of M 35/20, M 35/40 and N 60/20 concretes.

a positive indication of the hydration process and the presence of a dense microstructure contributing to the concrete's strength and durability. For the M 35/40 and M 60/20 concrete mixes, SEM images exhibited the formation of C-S-H gel at the bottom of the solid surface, showcasing an irregular net-like crystal structure. The SEM morphology of these blended mixes illustrated the development of a clear hardened phase, leading to the minimal presence of porosity. This characteristic results in a more compact nature of the concrete, indicating substantial bonding of the substrate. The negligible amount of porosity observed in these mixes signifies improved durability and resistance to environmental factors.

The SEM analysis thus provides valuable insights into the microstructural aspects of the concrete mixes, emphasizing the formation of C-S-H gel and the development of hardened phases. These findings are essential for understanding the concrete's mechanical and durability properties, contributing to the optimization of mix designs for enhanced performance in structural applications. The observed microstructural characteristics suggest that the M 35/40 and M 60/20 blended mixes exhibit favorable attributes, indicating their potential for applications requiring high strength and durability.

4. Summary for practical applications

The findings from the petrographic and mechanical studies of the aggregates and concrete mixes can significantly enhance concrete design, particularly when considering different environmental conditions. Some of the insights are highlighted for practical applications.

Utilizing hematite aggregates can significantly prolong the lifespan of concrete in areas exposed to high chloride levels, such as coastal regions. This characteristic makes it particularly suitable for marine constructions and roads subjected to de-icing salts. Moreover, hematite aggregates are advantageous for radiation shielding in nuclear facilities and pharmaceutical manufacturing units.

- Concrete mixtures that incorporate mineral additives alongside hematite aggregates exhibit improved split tensile and flexural strength, making them ideal for high-strength structural applications. This is especially critical in seismic zones where resistance to tensile and flexural forces is essential.
- Concrete mixes with a higher Young's modulus demonstrate an ability to resist stresses caused by temperature fluctuations, which is beneficial in regions with significant thermal variation. The dense microstructure contributes to minimizing cracking due to thermal expansion and contraction.
- Integrating mineral additives like low calcium FA and SF not only enhances mechanical properties but also promotes sustainability by lowering the carbon footprint of concrete. This approach aligns with eco-conscious design practices aimed at minimizing environmental impact.
- The mechanical property trends can be used to develop predictive models for long-term performance under varying environmental conditions, aiding in the design of maintenance and inspection schedules for infrastructure.

5. Conclusion

This study provides a detailed analysis of high-performance concrete using charnockite and hematite aggregates, focusing on their petrographic characteristics and mechanical performance. The comprehensive experimentation conducted in this study unravels critical insights into the determinants of Young’s modulus of concrete, paving the way for informed and sustainable concrete mix designs. Three pivotal factors such as the maximum size of aggregate, cement content, and the trade group of aggregate emerge as decisive influencers in achieving higher Young’s modulus.

- Comparing mixes with varying maximum aggregate sizes (M-2 and M-4), it becomes evident that minimizing cement content while maximizing aggregate size yields both the required compressive strength and Young’s modulus. However, practical considerations limit the use of larger (40 mm) aggregates in certain applications due to potential defects and challenges in concrete placement.
- A comprehensive examination of normal concrete mixes (M-3 to M-4) underscores the influence of higher cement content on achieving elevated compressive strength and Young's modulus. The strategic use of fillers and the optimization of paste content contribute significantly to enhancing Young’s modulus. The M 50/20 mixes exhibited cylindrical compressive strengths of 51.97 MPa, a 27% increase compared to M 35/20 mixes.
- The significance of aggregate type, with mixes (H-1 to H-3) featuring hematite (meta-sedimentary) aggregates demonstrating higher Young’s modulus and compressive strength. Quality of aggregate emerges as a key determinant, illustrated by the comparison between H-1 (H 35/20-heavy density concrete, 35 MPa and 20 mm maximum size of aggregate) and M-10 (M 60/20, 60 MPa concrete and maximum size of aggregate is 20 mm). Even with lower cement content, the Young’s modulus achieved is comparable to M60 grade, emphasizing the crucial role of aggregate quality.
- Young's modulus values ranged from 32.05 GPa to 40.16 GPa, with higher grades showing a 25% increase in stiffness. the maximum Young's modulus achieved was 40.16 GPa for the NC M 50/20 and 42.12 GPa for the MAC H 30/20.
- For conventional concrete mixes, tensile strength values increased with concrete grade, M 50/20 mixes achieving up to 3.96 MPa with 32% increase compared to M 35/20 mixes. Further, SEM analysis revealed a dense microstructure in M 35/20 mix, with negligible porosity (less than 5%), indicating enhanced durability.
- The MAC H 30/20 exhibited 15.74% increase in split tensile strength, 26.05% increase in flexural strength, and 16.48% increase in compressive strength compared to the NC

M 50/20.

In conclusion, the study demonstrates that the judicious selection of aggregates and the incorporation of mineral additives can significantly enhance the mechanical properties and durability of concrete. The results indicate that using hematite aggregates in combination with mineral additives can lead to concrete with up to 32% higher compressive strength and improve overall structural performance, making it suitable for demanding construction applications.

Acknowledgements

The authors also acknowledge the support provided by the Department of Quality Assurance and Control, L & T Construction, Chennai, India. The research team would like to thank office of Research and Development, ISO Labs for their research support.

Conflict of Interest

There is no conflict of interest.

Supporting Information

Applicable.

References

[1] H. Beushausen, T. Dittmer, The influence of aggregate type on the strength and elastic modulus of high strength concrete, *Construction and Building Materials*, 2015, **74**, 132-139, doi: 10.1016/j.conbuildmat.2014.08.055.

[2], S. N. Mahdi, T. Imjai, C. Wattanapanich, R. Garcia, H. Kaur, M. Ali Musarat, Life cycle cost analysis of flexible pavements reinforced with geo-synthetics: a case study of new construction or repair overlays in Thailand's Roads, *Engineered Science*, 2024, **28**, 1071, doi: 10.30919/es1071.

[3] M. Pasetto, N. Baldo, Mix design and performance analysis of asphalt concretes with electric arc furnace slag, *Construction and Building Materials*, 2011, **25**, 3458-3468, doi: 10.1016/j.conbuildmat.2011.03.037.

[4] Q. Dong, G. Wang, X. Chen, J. Tan, X. Gu, Recycling of steel slag aggregate in Portland cement concrete: an overview, *Journal of Cleaner Production*, 2021, **282**, 124447, doi: 10.1016/j.jclepro.2020.124447.

[5] K. Kishore, A. Pandey, N. K. Wagri, A. Saxena, J. Patel, A. Al-Fakih, Technological challenges in nanoparticle-modified geopolymer concrete: a comprehensive review on nanomaterial dispersion, characterization techniques and its mechanical properties, *Case Studies in Construction Materials*, 2023, **19**, e02265, doi: 10.1016/j.cscm.2023.e02265.

[6] I. H. Aziz, M. M. Al Bakri Abdullah, M. A. A. M. Salleh, L. Y. Ming, L. Y. Li, A. V. Sandu, P. Vizureanu, O. Nemes, S. N. Mahdi, Recent developments in steelmaking industry and potential alkali activated based steel waste: a comprehensive review, *Materials*, 2022, **15**, 1948, doi: 10.3390/ma15051948.

[7] J. Silvestre, N. Silvestre, J. de Brito, Review on concrete nanotechnology, *European Journal of Environmental and Civil Engineering*, 2016, **20**, 455-485, doi: 10.1080/19648189.2015.1042070.

[8] P. Tamayo, G. G. del Angel, J. Setién, A. Soto, C. Thomas, Feasibility of silicomanganese slag as cementitious material and as aggregate for concrete, *Construction and Building Materials*, 2023, **364**, 129938, doi: 10.1016/j.conbuildmat.2022.129938.

[9] S. N. Mahdi, D. V. Babu R, M. Shivakumar, M. M. Al Bakri Abdullah, Mitigation of environmental problems using brick kiln rice husk ash in geopolymer composites for sustainable development, *Current Research in Green and Sustainable Chemistry*, 2021, **4**, 100193, doi: 10.1016/j.crgsc.2021.100193.

[10] B. S. Thomas, S. Kumar, H. S. Arel, Sustainable concrete containing palm oil fuel ash as a supplementary cementitious material–A review, *Renewable and Sustainable Energy Reviews*, 2017, **80**, 550-561, doi: 10.1016/j.rser.2017.05.128.

[11] J. Chen, S.-C. Kou, C.-S. Poon, Hydration and properties of nano-TiO_2 blended cement composites, *Cement and Concrete Composites*, 2012, **34**, 642-649, doi: 10.1016/j.cemconcomp.2012.02.009.

[12] P. Dinakar, S. N. Manu, Concrete mix design for high strength self-compacting concrete using metakaolin, *Materials & Design*, 2014, **60**, 661-668, doi: 10.1016/j.matdes.2014.03.053.

[13] D. Hwangbo, D.-H. Son, H. Suh, J. Sung, B.-I. Bae, S. Bae, H. So, C.-S. Choi, Effect of nanomaterials (carbon nanotubes, nano-silica, graphene oxide) on bond behavior between concrete and reinforcing bars, *Case Studies in Construction Materials*, 2023, **18**, e02206, doi: 10.1016/j.cscm.2023.e02206.

[14] H. Yang, M. Monasterio, H. Cui, N. Han, Experimental study of the effects of graphene oxide on microstructure and properties of cement paste composite, *Composites Part A: Applied Science and Manufacturing*, 2017, **102**, 263-272, doi: 10.1016/j.compositesa.2017.07.022.

[15] F. Y. Al-saffar, L. S. Wong, S. C. Paul, An elucidative review of the nanomaterial effect on the durability and calcium-silicate-hydrate (C-S-H) gel development of concrete, *Gels*, 2023, **9**, 613, doi: 10.3390/gels9080613.

[16] E. J. Garboczi, Concrete Nanoscience and Nanotechnology: Definitions and Applications. Z. Bittnar, P. J. M. Bartos, J. Němeček, V. Šmilauer, J. Zeman, Eds., Nanotechnology in Construction 3 Springer Berlin Heidelberg, Berlin, Heidelberg, 2009.

[17] M. Jalal, E. Mansouri, M. Sharifipour, A. R. Pouladkhan, Mechanical, rheological, durability and microstructural properties of high performance self-compacting concrete containing SiO_2 micro and nanoparticles, *Materials & Design*, 2012, **34**, 389-400, doi: 10.1016/j.matdes.2011.08.037.

[18] M. Z. Y. Ting, K. S. Wong, M. E. Rahman, M. Selowara Joo, Mechanical and durability performance of marine sand and seawater concrete incorporating silicomanganese slag as coarse aggregate, *Construction and Building Materials*, 2020, **254**, 119195, doi: 10.1016/j.conbuildmat.2020.119195.

[19] M. J. Shannag, Characteristics of lightweight concrete containing mineral admixtures, *Construction and Building Materials*, 2011, **25**, 658-662, doi: 10.1016/j.conbuildmat.2010.07.025.

[20] X. H. Wu, P. Yuan, Y. T. Jiao, Influence of fly ash as cement replacement on chloride penetration and frost resistance of recycled concrete, *Advanced Materials Research*, 2011, **250-253**, 1031-1037, doi: 10.4028/www.scientific.net/amr.250-253.1031.
[21] Z. Li, L.-Y. Li, S. Cheng, Evaluation of modulus of elasticity of concrete containing both natural and recycled concrete aggregates, *Journal of Cleaner Production*, 2024, **447**, 141591, doi: 10.1016/j.jclepro.2024.141591.
[22] W.-B. Yuan, L. Mao, L.-Y. Li, A two-step approach for calculating chloride diffusion coefficient in concrete with both natural and recycled concrete aggregates, *Science of the Total Environment*, 2023, **856**, 159197, doi: 10.1016/j.scitotenv.2022.159197.
[23] A. K. Padmini, K. Ramamurthy, M. S. Mathews, Influence of parent concrete on the properties of recycled aggregate concrete, *Construction and Building Materials*, 2009, **23**, 829-836, doi: 10.1016/j.conbuildmat.2008.03.006.
[24] G. Giaccio, R. Zerbino, Failure Mechanism of Concrete: Combined effects of coarse aggregates and strength level, *Advanced Cement Based Materials*, 1998, **7**, 41-48, doi: 10.1016/S1065-7355(97)00014-X.
[25] M. Uysal, The influence of coarse aggregate type on mechanical properties of fly ash additive self-compacting concrete, *Construction and Building Materials*, 2012, **37**, 533-540, doi: 10.1016/j.conbuildmat.2012.07.085.
[26] A. Kılıç, C. D. Atiş, A. Teymen, O. Karahan, F. Özcan, C. Bilim, M. Özdemir, The influence of aggregate type on the strength and abrasion resistance of high strength concrete, *Cement and Concrete Composites*, 2008, **30**, 290-296, doi: 10.1016/j.cemconcomp.2007.05.011.
[27] A. M. Rashad, A comprehensive overview about the effect of nano-SiO_2 on some properties of traditional cementitious materials and alkali-activated fly ash, *Construction and Building Materials*, 2014, **52**, 437-464, doi: 10.1016/j.conbuildmat.2013.10.101.
[28] Y. Zhou, Z. Zhang, Effect of fineness on the pozzolanic reaction kinetics of slag in composite binders: experiment and modelling, *Construction and Building Materials*, 2021, **273**, 121695, doi: 10.1016/j.conbuildmat.2020.121695.
[29] Y.-S. Wang, Y. Alrefaei, J.-G. Dai, Influence of coal fly ash on the early performance enhancement and formation mechanisms of silico-aluminophosphate geopolymer, *Cement and Concrete Research*, 2020, **127**, 105932, doi: 10.1016/j.cemconres.2019.105932.
[30] T. Wang, T. Ishida, R. Gu, Y. Luan, Experimental investigation of pozzolanic reaction and curing temperature-dependence of low-calcium fly ash in cement system and Ca-Si-Al element distribution of fly ash-blended cement paste, *Construction and Building Materials*, 2021, **267**, 121012, doi: 10.1016/j.conbuildmat.2020.121012.
[31] L. P. Singh, S. R. Karade, S. K. Bhattacharyya, M. M. Yousuf, S. Ahalawat, Beneficial role of nanosilica in cement based materials–A review, *Construction and Building Materials*, 2013, **47**, 1069-1077, doi: 10.1016/j.conbuildmat.2013.05.052.
[32] J. Z. Chong, N. M. Sutan, I. Yakub, Characterization of early pozzolanic reaction of calcium hydroxide and calcium silicate hydrate for nanosilica modified cement paste, *Journal of Civil Engineering, Science and Technology*, 2013, **4**, 6-10, doi: 10.33736/jcest.120.2013.
[33] G. Shakhmenko, I. Juhnevica, A. Korjakins, Influence of sol-gel nanosilica on hardening processes and physically-mechanical properties of cement paste, *Procedia Engineering*, 2013, **57**, 1013-1021, doi: 10.1016/j.proeng.2013.04.128.
[34] N. R. Rakhimova, R. Z. Rakhimov, Reaction products, structure and properties of alkali-activated metakaolin cements incorporated with supplementary materials–a review, *Journal of Materials Research and Technology*, 2019, **8**, 1522-1531, doi: 10.1016/j.jmrt.2018.07.006.
[35] M. Balapour, A. Joshaghani, F. Althoey, Nano-SiO_2 contribution to mechanical, durability, fresh and microstructural characteristics of concrete: a review, *Construction and Building Materials*, 2018, **181**, 27-41, doi: 10.1016/j.conbuildmat.2018.05.266.
[36] S. Shahbazpanahi, R. H. Faraj, Feasibility study on the use of shell sunflower ash and shell pumpkin ash as supplementary cementitious materials in concrete, *Journal of Building Engineering*, 2020, **30**, 101271, doi: 10.1016/j.jobe.2020.101271.
[37] R. T.-Ncm, Application of nanotechnology in construction. Summary of a state-of-the-art report, *Materials and Structures*, 2004, **37**, 649-658, doi: 10.1617/14234.
[38] C. Shi, Z. Wu, J. Xiao, D. Wang, Z. Huang, Z. Fang, A review on ultra-high performance concrete: part I. Raw materials and mixture design, *Construction and Building Materials*, 2015, **101**, 741-751, doi: 10.1016/j.conbuildmat.2015.10.088.
[39] N. M. Azmee, N. Shafiq, Ultra-high-performance concrete: from fundamental to applications, *Case Studies in Construction Materials*, 2018, **9**, e00197, doi: 10.1016/j.cscm.2018.e00197.
[40] R. H. Faraj, A. A. Mohammed, K. M. Omer, Synergistic effects of recycled plastic aggregate and nano-silica on the elevated temperature and durability performance of self-compacting concrete, *Journal of Building Engineering*, 2023, **75**, 106986, doi: 10.1016/j.jobe.2023.106986.
[41] R. H. Faraj, A. A. Mohammed, K. M. Omer, Microstructure characteristics, stress–strain behaviour, fresh properties, and mechanical performance of recycled plastic aggregate self-compacting concrete modified with nano-silica, *Construction and Building Materials*, 2023, **383**, 131371, doi: 10.1016/j.conbuildmat.2023.131371.
[42] Z. Zhao, T. Qi, W. Zhou, D. Hui, C. Xiao, J. Qi, Z. Zheng, Z. Zhao, A review on the properties, reinforcing effects, and commercialization of nanomaterials for cement-based materials, *Nanotechnology Reviews*, 2020, **9**, 303-322, doi: 10.1515/ntrev-2020-0023.
[43] B. Liu, X. Lu, H. Meng, G. Pan, D. Li, Dispersion of *in situ* controllably grown nano-SiO_2 in alkaline environment for improving cement paste, *Construction and Building Materials*, 2023, **369**, 130460, doi: 10.1016/j.conbuildmat.2023.130460.
[44] Bureau of Indian Standard, "IS 269", Ordinary Portland Cement – Specification, India, 2015.
[45] Bureau of Indian Standard, "IS 2386", Methods of Test for

Aggregates for Concrete - Part I: Particle Size and Shape, 2019.
[46] Bureau of Indian Standard, “IS 3812”, Pulverized Fuel Ash - Part 1: For Use as Pozzolana in Cement, Cement Mortar and Concrete, 2013.
[47] Bureau of Indian Standard, “IS 15388”, Specification for Silica Fume, 2003.
[48] Bureau of Indian Standard, “IS 10262”, Concrete Mix Proportioning - Guidelines, 2019.
[49] M. Beyene, R. Meininger, J. F. Munoz, Mineralogic and petrographic evaluation of aggregate quality–effect on compressive strength of concrete pavement, *International Journal of Pavement Engineering*, 2023, **24**, 1-15, doi: 10.1080/10298436.2022.2088756.
[50] H. T. Dinesh, M. Shivakumar, M. S. Dharmaprakash, R. V. Ranganath, Influence of reactive SiO_2 and Al_2O_3 on mechanical and durability properties of geopolymers, *Asian Journal of Civil Engineering*, 2019, **20**, 1203-1215, doi: 10.1007/s42107-019-00167-5.
[51] C. Telloli, A. Aprile, E. Marrocchino, Petrographic and physical-mechanical investigation of natural aggregates for concrete mixtures, *Materials*, 2021, **14**, 5763, doi: 10.3390/ma14195763.
[52] W. Zhong, J. Pan, J. Wang, C. Zhang, Size effect in dynamic splitting tensile strength of concrete: experimental investigation, *Construction and Building Materials*, 2021, **270**, 121449, doi: 10.1016/j.conbuildmat.2020.121449.
[53] P. Jagadesh, A. Juan-Valdés, M. I. Guerra-Romero, J. M. Morán-del Pozo, J. García-González, R. Martínez-García, Effect of design parameters on compressive and split tensile strength of self-compacting concrete with recycled aggregate: an overview, *Applied Sciences*, 2021, **11**, 6028, doi: 10.3390/app11136028.
[54] L. Jin, W. Yu, X. Du, Size effect on static splitting tensile strength of concrete: experimental and numerical studies, *Journal of Materials in Civil Engineering*, 2020, **32**, 04020308, doi: 10.1061/(asce)mt.1943-5533.0003382.
[55] L. Burhan, K. Ghafor, A. Mohammed, Quantification the effect of microsand on the compressive, tensile, flexural strengths, and modulus of elasticity of normal strength concrete, *Geomechanics and Geoengineering*, 2021, **16**, 478-496, doi: 10.1080/17486025.2019.1680884.
[56] M. Orouji, S. M. Zahrai, E. Najaf, Effect of glass powder & polypropylene fibers on compressive and flexural strengths, toughness and ductility of concrete: an environmental approach, *Structures*, 2021, **33**, 4616-4628, doi: 10.1016/j.istruc.2021.07.048.
[57] C. Sreenivasulu, J. Guru Jawahar, C. Sashidhar, Effect of copper slag on micro, macro, and flexural characteristics of geopolymer concrete, *Journal of Materials in Civil Engineering*, 2020, **32**, 04020086, doi: 10.1061/(asce)mt.1943-5533.0003157.
[58] M.-C. Kang, D.-Y. Yoo, R. Gupta, Machine learning-based prediction for compressive and flexural strengths of steel fiber-reinforced concrete, *Construction and Building Materials*, 2021, **266**, 121117, doi: 10.1016/j.conbuildmat.2020.121117.
[59] S. N. Mahdi, D. V. Babu R, N. Hossiney, M. M. Al Bakri Abdullah, Strength and durability properties of geopolymer paver blocks made with fly ash and brick kiln rice husk ash, *Case Studies in Construction Materials*, 2022, **16**, e00800, doi: 10.1016/j.cscm.2021.e00800.
[60] H. Bahmani, D. Mostofinejad, Microstructure of ultra-high-performance concrete (UHPC)–A review study, *Journal of Building Engineering*, 2022, **50**, 104118, doi: 10.1016/j.jobe.2022.104118.
[61] Bureau of Indian Standard, “IS 383”, Coarse and Fine Aggregate for Concrete - Specification, 2016.

